JOURNAL OF MATERIALS SCIENCE **39** (2004) 5825–5830

Sintering of tin oxide using zinc oxide as a densification aid

C. R. FOSCHINI
Department of Materials Science and Engineering, Virginia Polytechnic Institute and State University, Blacksburg, VA 24061-0237, USA
E-mail: cfoschini@mse.vt.edu

L. PERAZOLLI, J. A. VARELA
Institute of Chemistry, Universidade Estadual Paulista, UNESP, Araraquara, SP 14801-970, Brazil

The physicochemical electronic characteristics of SnO_2 render it useful in many technical applications, including ceramic varistors, stable electrodes used in electric glass-melting furnaces and electrometallurgy of aluminum, transparent windows and chemical sensors. The use of ZnO as a sintering aid was explored in this study to obtain SnO_2 as a dense ceramic. Compacts were obtained by mechanical mixing of oxides, isostatic pressing at 210 MPa and sintering *in situ* inside a dilatometer at heating rates of 10°C/min. The grain size and microstructure were investigated by scanning and transmission electron microscopy (SEM/TEM). The phases and chemical composition were analyzed by energy dispersive spectroscopy (EDS) and X-ray diffraction (XRD). The results indicated that ZnO acts as a densification aid for SnO_2, improving its grain growth with additions of up to 2 mol%. ZnO forms a solid solution with SnO_2 up to 1 mol%, above which $SnZnO_3$ precipitates in the grain boundary, potentially inhibiting shrinkage and grain growth.

1. Introduction

Much interest has focused on obtaining dense SnO_2 ceramics for applications such as varistors [1], photochemical devices [2], electrodes for electric glass-melting furnaces, and components requiring high chemical corrosion resistance [3, 4]. However, tin oxide ceramics show poor sinterability and sintering aids have been used to promote densification. Several authors have studied the effect of different oxides such as CoO [5], CuO [2–4, 6], ZnO [7, 8], MnO_2 [5, 8], Nb_2O_5 [9], V_2O_5 [10] and Sb_2O_3 [11] in SnO_2 sintering and densities of 94 to 99% of the theoretical value for SnO_2 have been obtained. Nevertheless, the sintering mechanism is still a controversial issue, for which [8] proposed a diffusion mechanism while [5] proposed the formation of oxygen vacancies given by:

$$MnO_2 \xrightarrow{SnO_2} Mn''_{Sn} + V^{\cdot\cdot}_O + O^x_O \quad (1)$$

$$CoO \xrightarrow{SnO_2} Co''_{Sn} + V^{\cdot\cdot}_O + O^x_O \quad (2)$$

SnO_2 and ZnO are *n*-type semiconductors with close ionic radii ($R^{+4}_{Sn} = 0.71$ Å and $R^{+2}_{Zn} = 0.74$ Å), tetragonal rutile-type and hexagonal compact structures, respectively. The difference in ionic charge, structures and ionic radii proximity suggest the use of ZnO as a densification aid for SnO_2 [12], considering the oxygen vacancy diffusion mechanisms proposed in Equations 1 and 2. Few reports describe the effect of sintering atmospheres or the role of ZnO on SnO_2 sintering. Grigoryan *et al*. [7] and Paria *et al*. [8] studied the sintering of ZnO-doped SnO_2 and found that ZnO acts as a densification agent for SnO_2. Paria *et al*. obtained an activation energy of 153 kJ/mol in the sintering of 1 mol% ZnO-doped SnO_2. Quadir and Readey [13] observed that sintering SnO_2 in a hydrogen atmosphere caused the compact to expand, decreasing its apparent density, and that the behavior of exaggerated particle growth was nonisotropic. They found that the expansion process was caused by agglomerate grain growth due to evaporation condensation at temperatures above 1200°C, which is given by the equation:

$$SnO_{2(s)} \rightarrow SnO + \frac{1}{2}O_2 \quad (3)$$

Perazolli *et al*. [14, 15] studied the influence of the atmosphere on SnO_2 plus ZnO sintering, verifying that Zn promotes densification due the formation of oxygen vacancies in the structure, which is expressed by Equation 4:

$$ZnO \xrightarrow{SnO_2} Zn''_{Sn} + V^{\cdot\cdot}_O + O^x_0 \quad (4)$$

The present study involved an investigation of the sintering behavior of the SnO_2-ZnO system. The fracture surface of sintered samples was analyzed by SEM,

while the grain boundary precipitates formed at the grain boundaries in compositions with ZnO content exceeding 2 mol% were analyzed by TEM. The predominant densification mechanism is suggested here, as is the probable formation of a $SnZnO_3$ phase at the grain boundaries.

2. Experimental procedure

The oxides used in this study were SnO_2, CESBRA (purity > 99.9%; mean particle size = 0.09 μm; 9.2 m^2/g surface area) and ZnO (purity > 99.0%; mean particle size = 0.21 μm; 5.0 m^2/g surface area). The powders were mechanically mixed in isopropyl alcohol for 30 min, using zirconia balls as the medium. SnO_2 was doped with 0 to 10 mol% of ZnO. After drying, the powders were granulated into pellets, which were compacted into 8 mm diameter cylindrical specimens and isostatically pressed at 210 MPa to a green density of 57–60% of the theoretical density (6.994 g/cm^3) [12]. The samples were sintered in a dilatometer (Model 402E NETZSCH Geratebau, Selb, Germany) up to 1500°C, at a constant heating rate of 10°C/min in a dry air sintering atmosphere. After measuring the sintered densities by the Archimedes method, the phases were analyzed by XRD (SIEMENS D5000). The microstructure of sintered pellets was characterized by SEM (TOPCON SM300) and TEM (Philips CM200), both coupled to energy-dispersive X-ray spectrometers (Princeton Gamma-Tech).

3. Results and discussion

Fig. 1a and b show the shrinkage versus temperature for SnO_2 powders doped with 0.5 to 5 mol% ZnO, sintered at 1500°C at a 10°C/min heating rate. Fig. 1a shows the results for linear shrinkage while Fig. 1b plots the linear shrinkage rate. Table I summarizes the results obtained. The TG/DTA results shown in Fig. 2a and b indicate that the ceramic powder obtained

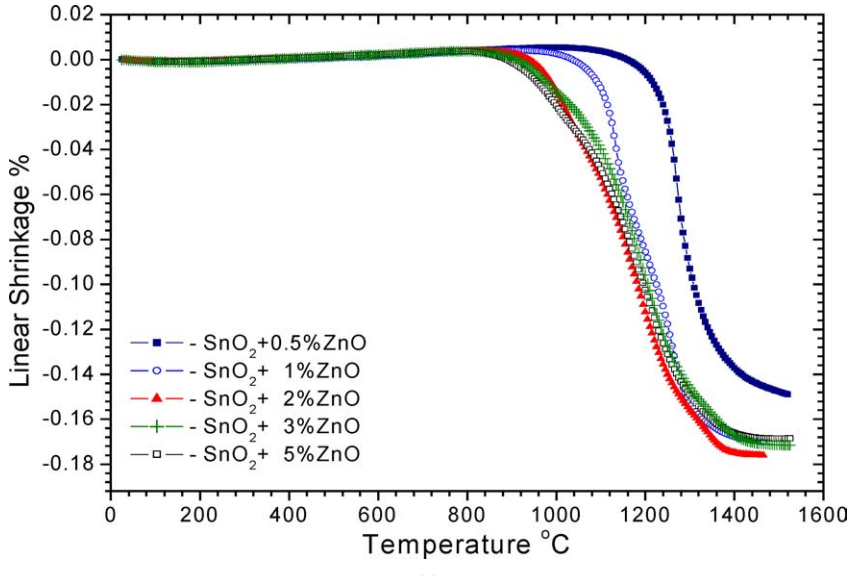

(a)

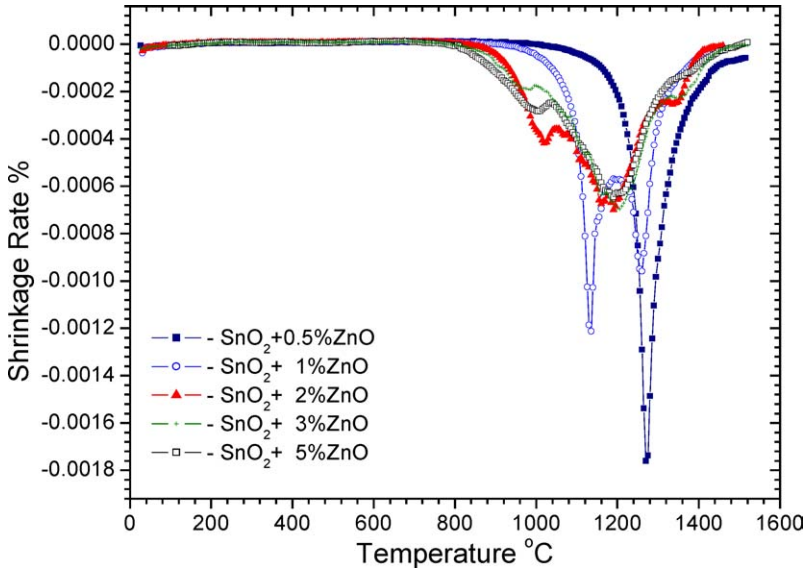

(b)

Figure 1 Dilatometric results obtained from ZnO-doped SnO_2 sintered at a 10°C/min heating rate up to 1500°C in dry air: (a) linear shrinkage and (b) shrinkage rate.

TABLE I Dilatometric results obtained during the sintering of SnO_2-ZnO samples at a constant heating rate. T_{sd} is the temperature at which densification begins; T_{max} is the temperature at which the shrinkage rate is at its maximum; $Y_{1450°C}$ is the shrinkage at 1450°C; G is the mean grain size; Q is the activation energy and ρ is the relative density

ZnO content (mol%)	T_{sd} (°C)	T_{max} (°C)	$Y_{1450°C}$ (°C)	G (μm)	Q (kJ/mol)	ρ (%)
0.5	875	1270	9.24	4.5	525	95.0
1.0	790	1135	16.98	6.1	457	97.1
2.0	770	1190	17.59	6.8	125	98.3
3.0	750	1205	17.07	5.3	135	97.0
5.0	755	1220	16.82	5.4	116	96.5

did not react chemically in the temperature range applied to sinter the pellets and that the peaks appearing at 1200°C in Fig. 2a were a attributable to a stannic reduction, according to Equation 3. Nevertheless, the pure SnO_2 system displayed no weight loss up to 1300°C. The weight loss occurring above 1200°C was due to the reduction of SnO_2 to SnO (Equation 3). The addition of ZnO led to the formation of oxygen vacancies (Equation 4) that competed with the O_2 formed, inhibiting the formation of SnO, according to Equation 3, and the starting temperature of weight loss shifted from 1200 to 1300°C. A constant weight gain occurred due

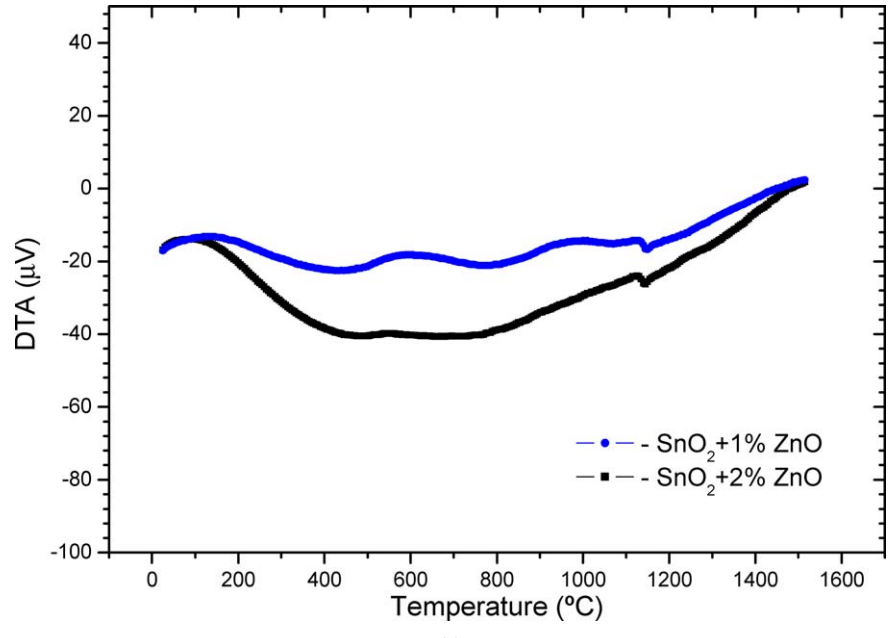

(a)

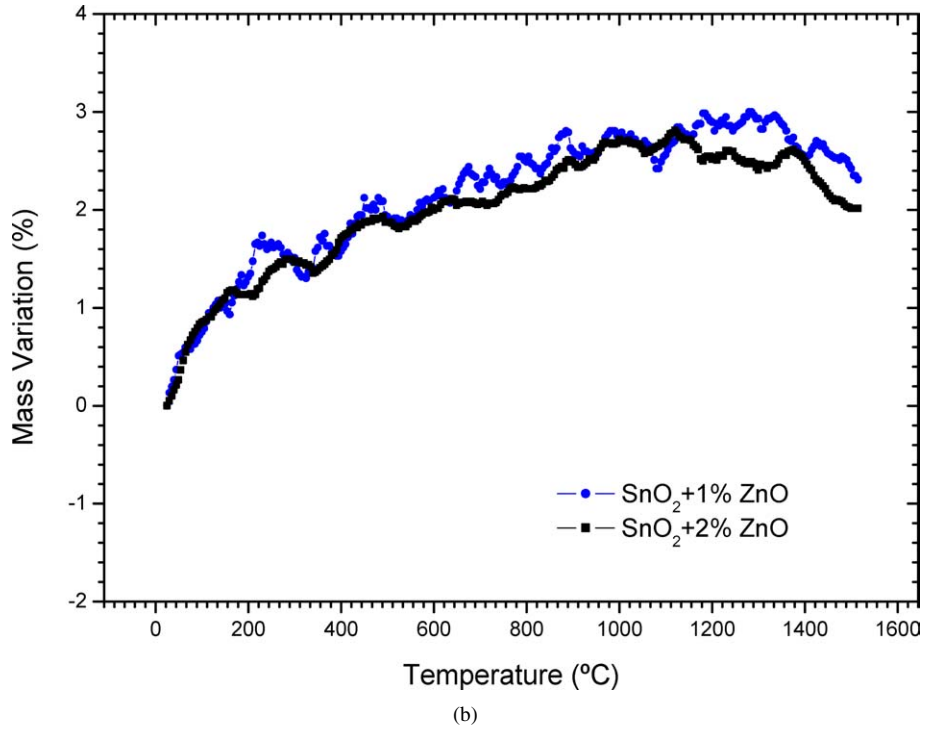

(b)

Figure 2 Thermal analysis results of ZnO-doped SnO_2 sintered at a heating rate of 10°C/min up to 1500°C in dry air: (a) DTA (b) TG.

to the absorption of O_2 up to 1300°C, after which the weight loss up to 1500°C was less than 1% in mass, due to the evaporation of SnO_2.

The thermal analysis and the dilatometric results indicate that ZnO acts as a SnO_2 densification agent and that increasing the ZnO concentration up to 2 mol% promotes a linear retraction, reducing the starting sintering temperature and activation energy of the process, calculated by the Bannister Method [16]. The ZnO acts as a densification aid by triggering the formation of oxygen vacancies. During the sintering of ZnO-doped SnO_2, according to Equation 4, the vacancies cause the material to diffuse. Not only the vacancies but also the expansion of the unit cell due to the higher ionic radii of Zn^{2+}(74 Å) compared with the ionic radii of Sn^{4+}(45 Å) may promote material or atomic diffusion in the crystal lattice.

In this study, the system's sintering process was divided into 4 different stages: I—pre-initial; II—initial; III—intermediate and IV—final. For the pre-initial stage, a linear shrinkage mechanism was established, caused by the structural rearrangement of particles with viscous flow characteristics, since no liquid phase formation was detected in this range of temperature. The sintering mechanism for the initial stage was not identified because of the probable combination of two or more different densification and nondensification mechanisms acting simultaneously. Though not identified, the action of the same sintering mechanism was evidenced for the initial stage, independently of the ZnO concentration.

The linear shrinkage/densification observed was likely attributable to the generation of oxygen vacancies, as expressed by Equation 4.

The linear shrinkage behavior as a function of temperature in all the compositions illustrated in Fig. 1 displayed a sigmoidal shape, indicating that the final stage of sintering was reached. However, from Fig. 1b one can see that, up to 1 mol% of ZnO, the curves do not present shoulders or anomalies, indicating the formation of solid solution between SnO_2-ZnO. For ZnO concentrations of more than 1 mol%, two shoulders before and after the temperature of maximum linear shrinkage rate are visible. The first shoulder indicates the occurrence of intergranular sintering due to the difference in particle size between SnO_2 and ZnO. The second shoulder indicates the occurrence of mobility impediments at the grain boundary's solid-solid interface, which may be attributed to the formation of a precipitated ZnO-rich phase at the grain boundaries. The sintering curve for the 1 mol% concentration differs from the other curves, showing two peaks in the temperature region of maximum linear shrinkage. These results and the SEM/TEM analyses suggest that the 1 mol% concentration is close to the solid solution limit for the SnO_2-ZnO system.

The micrographs of the fractured samples, Fig. 3, illustrate the residual porosity of the 0.5 mol% ZnO sample and the formation of precipitates at the grain

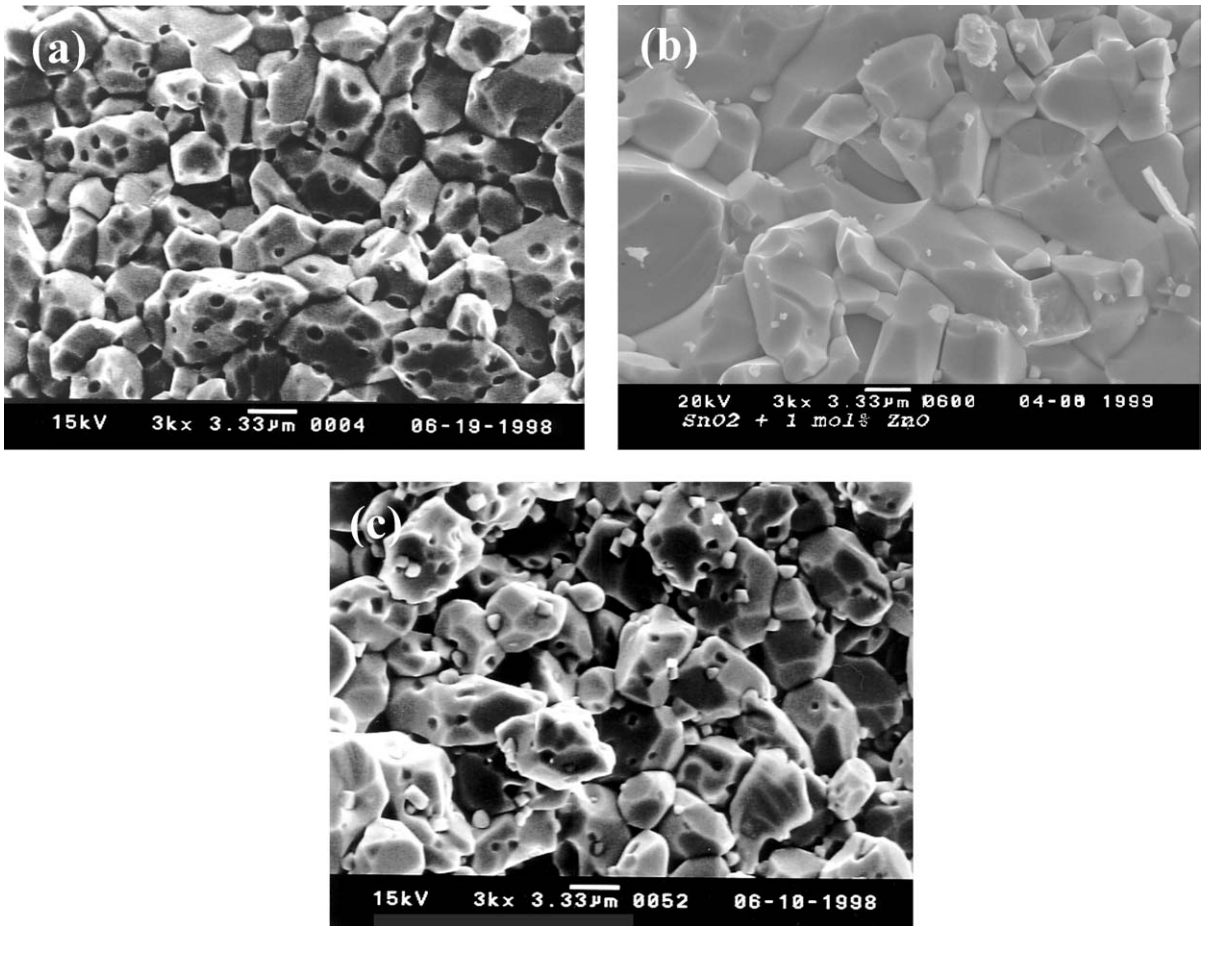

Figure 3 SEM micrographs of fractured samples with ZnO content of: (a) 0.5 mol%, (b) 1.0 mol% and (c) 5 mol% ZnO.

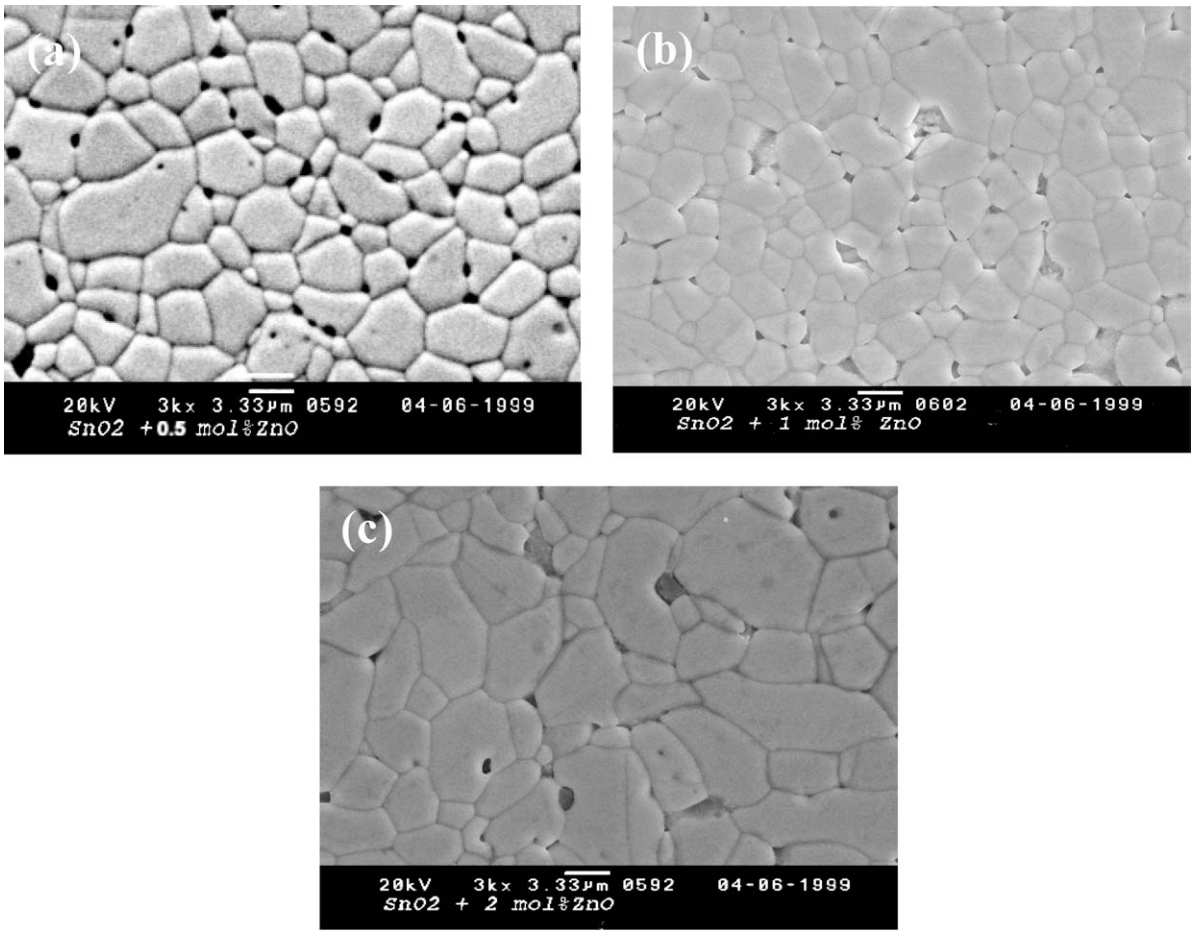

Figure 4 SEM micrographs of polished and thermally etched samples with ZnO content of: (a) 0.5 mol%, (b) 1.0 mol% and (c) 2 mol% ZnO.

boundaries in compositions whose ZnO content exceeds 1 mol%. These precipitates can inhibit the advance of grain growth during the intermediate sintering stage.

Fig. 4 shows micrographs of the samples' surfaces after the polishing and thermal etching applied to determine the average grain size. The average grain size in samples with a ZnO content of 0.5 to 5 mol% ranged from 4.5 to 6.8 μm (see Table I).

An analysis was made of the composition of the grain boundary inclusions using EDS coupled to a TEM microscope. Fig. 5a and b show a micrograph and an energy dispersive spectrum of a sample containing 5 mol% ZnO. A chemical analysis of the darker grains in these samples revealed a ZnO-rich phase, as illustrated in Fig. 5b, when compared with the brighter region. This ZnO-rich phase was identified as $SnZnO_3$ through an XRD analysis of samples with 10 mol% ZnO, as depicted in Fig. 6. Samples containing less than 1 mol% ZnO did not exhibit the presence of any precipitate at the grain boundaries, indicating the formation of solid solution between ZnO and SnO_2.

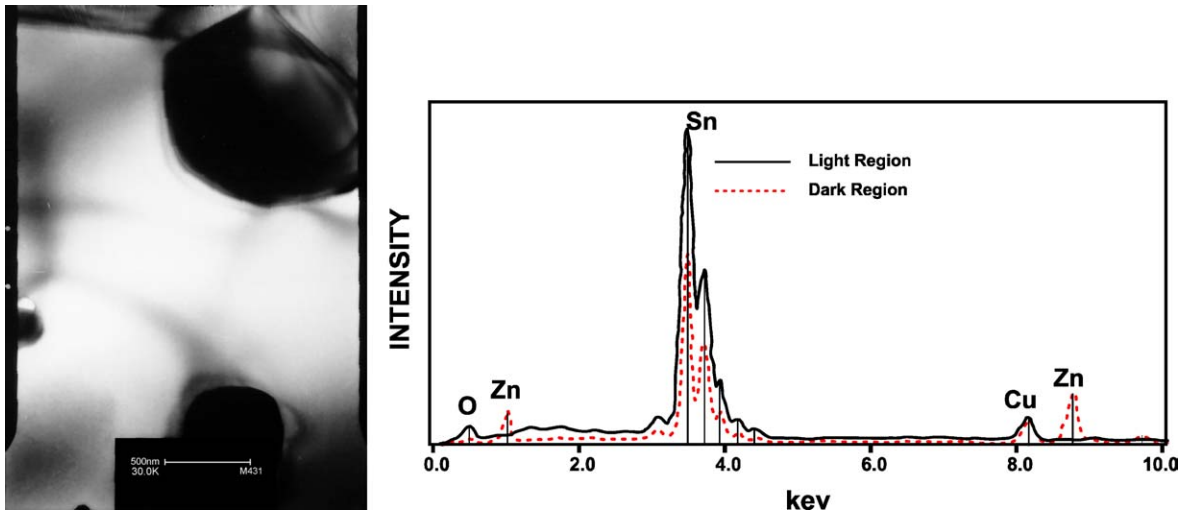

Figure 5 TEM micrograph and EDS spectrum of a sample containing 5 mol% ZnO.

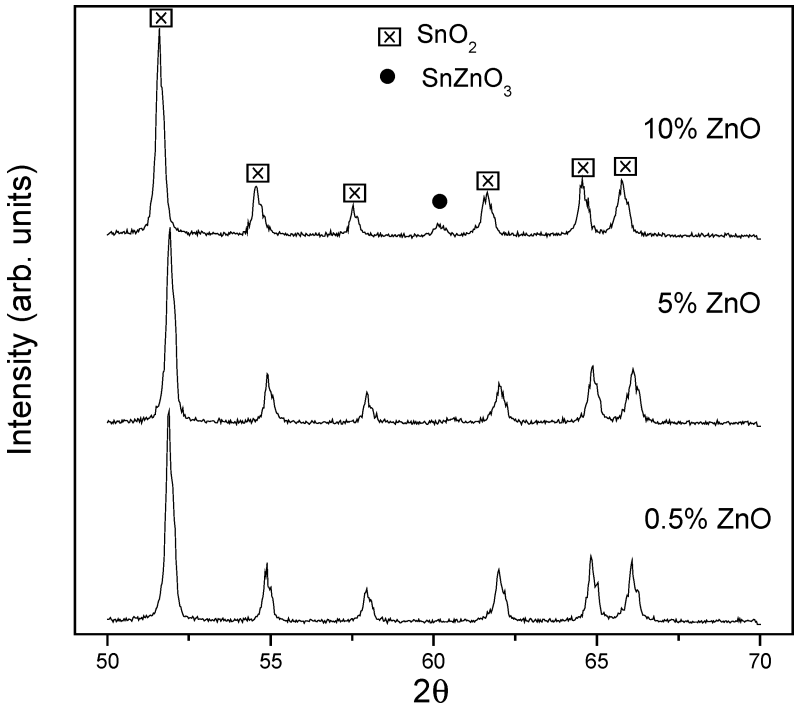

Figure 6 XRD patterns of ZnO-doped SnO_2 samples with different ZnO contents.

The presence of an $SnZnO_3$ phase precipitated at the grain boundaries in samples with ZnO content exceeding 1 mol% may act as a barrier, preventing grain boundary motion and inhibiting densification, as observed in Figs 3, 4 and 5.

The peak shift observed by XRD (Fig. 6) in the SnO_2 phase with a larger amount of ZnO may be attributed to changes in the lattice parameters of the SnO_2 crystalline phase. Increasing the amount of ZnO, which transforms substitutional solid solution into SnO_2, causes an expansion of the unit cell due to the higher ionic radii of Zn^{2+} (0.74 Å) compared with those of Sn^{4+} (0.69 Å), and the additional Zn promotes the expulsion of one oxygen atom, leading to a cationic repulsion between the nearest neighbor atoms around the oxygen vacancy. Fig. 6 also shows the formation of $SnZnO_3$ phase, which was confirmed by the presence of a peak at $2\theta \cong 60^{\circ}$ in samples containing 10 mol% of ZnO.

4. Conclusions

ZnO acts as a densifying agent for SnO_2 through the oxygen vacancy formation mechanism. The use of ZnO as a densification agent, using conventional sintering techniques, results in dense SnO_2.

ZnO promotes SnO_2 sinterability, allowing one to obtain samples with final densities of over 98%. The formation of a single phase solid solution was observed in SnO_2 samples with up to 1 mol% ZnO. Samples with higher ZnO content displayed the presence of a $SnZnO_3$ phase precipitated at the grain boundaries, which may act as a barrier for grain mobility, inhibiting densification and grain growth.

Acknowledgements

The authors gratefully acknowledge the comments and suggestions of Dr. W. S. Coblenz from the Defense Advanced Research Projects Agency-DARPA and the financial support of the Brazilian research funding institutions CNPq, CAPES and FAPESP.

References

1. S. A. PIANARO, P. R. BUENO, E. LONGO and J. A. VARELA, *J. Mater. Sci. Lett.* **14** (1995) 692.
2. Z. M. JARZEBSKI and J. P. MARTON, *J. Electrochem. Soc.: Reviews and News* (1976).
3. M. ZAHARESCU, S. MIHAIU, S. ZUCA and K. MATIASOVSKY, *J. Mater. Sci.* **26** (1991) 1666.
4. Z. M. JARZEBSKI and J. P. MARTON, *J. Electrochem. Soc.: Reviews and News* (1976) 199C.
5. J. A. CERRI, E. R. LEITE, D. GOUVÊA and E. LONGO, *J. Amer. Ceram. Soc.* **79**(5) (1996) 799.
6. S. A. PIANARO, P. R. BUENO, E. LONGO and J. A. VARELA, *J. Mater. Sci. Lett.* **14** (1995) 692.
7. L. T. GRIGORYAN, Z. H. GEDAKYAN and K. A. KOSTANYAU, *Inorg. Mater.* **12** (1974) 313.
8. M. K. PARIA, S. BASU and A. PAUL, *Trans. Indian Ceram. Soc.* **42**(4) (1983) 90.
9. J. TAKAHASHI, I. YAMAI and H. SAITO, *Yogyo Kyokaishi* **83**(7) (1975) 362.
10. J. TAKAHASHI, K. KODAIRA, T. MATSUSHITA, I. YAMAI and H. SAITO, *ibid.* **83**(1) (1975) 33.
11. T. MATSUSHITA and I. YAMAI, *ibid.* **80**(8) (1972) 305.
12. Powder Diffraction File, Cards No. 21-1250 and 41-1445, Joint Committee on Powder Diffraction Standards, Swarthmore, PA.
13. T. QUADIR and D. W. READEY, in "Microstructure Evolution in SnO_2 and CdO in Reducing Atmosphere in Sintering and Heterogeneous us Catalysis," edited by G. C. Kuczynsdi (Plenum Publ. Co., 1984).
14. L. PERAZOLLI, C. R. FOSCHINI, T. R. GIRALDI, R. S. BISCARO, J. A. VARELA and E. LONGO, *Sinter. Sci. Techn.* (2000) 117.
15. L. PERAZOLLI, J. A. VARELA, E. R. LEITE and E. LONGO, *Mater. Sci. Forum* **v.299/300** (1999) 134.
16. J. L. WOOLFREY and M. J. BANNISTER, *J. Amer. Ceram. Soc.* **55**(8) (1972) 390.

Received 17 January 2003
and accepted 6 April 2004